Available online at www.sciencedirect.com
ScienceDirect
International Journal of Mass Spectrometry 262 (2007) 220–231
International Journal of Mass Spectrometry
www.elsevier.com/locate/ijms

Definitive evidence for the existence of isomeric chlorophenyl radicals ($C_6H_4Cl^{\bullet}$) from charge inversion mass spectrometry and DFT calculations

Shigeo Hayakawa *, Hiroshi Matsubara, Yoshiaki Kawamura, Kenichi Iwamoto

Department of Chemistry, Graduate School of Science, Osaka Prefecture University, 1-1, Gakuen-cho, Nakaku, Sakai, Osaka 599-8531, Japan

Received 26 September 2006; received in revised form 23 November 2006; accepted 23 November 2006
Available online 27 December 2006

Abstract

Free radical species are much more reactive than stable molecules, and so usually exist only as transient intermediates in chemical reactions. Charge inversion mass spectrometry using alkali metal targets is an effective method for determining the structure and dissociation processes of radicals, and can also enable differentiation between isomeric forms of compounds whose parent ions have similar mass spectra and similar collisionally activated dissociation spectra, such as the isomers of dichlorobenzene and chlorophenol. The charge inversion process using alkali metal targets proceeds via near-resonant neutralization, followed by spontaneous dissociation of the excited neutrals, and then endothermic negative ion formation. In the normalized charge inversion spectra of *ortho*-, *meta*-, and *para*-dichlorobenzene ($C_6H_4Cl_2$) measured in this work, the intensities of the peaks associated with chlorine anions (Cl^-) are almost same for each of the isomers, whereas the intensities of the peaks associated with the chlorophenyl anions ($C_6H_4Cl^-$) display a strong dependence on the isomeric structure of the parent compound. The similarities of the Cl^- ion peak intensities indicate that neutralization cross-sections and branching ratios to produce Cl radicals are the same for each of the isomeric precursor $C_6H_4Cl_2^+$ ions. The strong isomer-dependence of the peak intensities of $C_6H_4Cl^-$ anions suggests that the chlorophenyl radicals ($C_6H_4Cl^{\bullet}$) formed from $C_6H_4Cl_2$ by loss of Cl do not undergo isomerization, and that the electron transfer cross-sections to form the negative ions are strongly isomer-dependent. Density functional theory (DFT) calculations on the *o*-, *m*-, and *p*-$C_6H_4Cl^{\bullet}$ radicals show that the barriers to isomerization are in excess of 2.8 eV, and these high isomerization barriers are believed to be the reason for the absence of isomerization among the $C_6H_4Cl^{\bullet}$ radicals during the charge inversion process. Calculated adiabatic electron affinities and vertical electron affinities both show differences for the *o*-, *m*-, and *p*-isomers, but the trend in the magnitude of the electron affinities has an inverse relation to the peak intensities of the isomeric $C_6H_4Cl^-$ ions in the charge inversion spectra. It is, therefore, assumed that the cross-sections for negative ion formation are influenced by many factors other than the electron affinity, such as the relatively large geometrical distortion in the chlorophenyl radicals predicted in this work. The good agreement between the experimental results and the theoretical predictions obtained in this work provides compelling evidence for the existence of isomeric $C_6H_4Cl^{\bullet}$ radicals that do not undergo isomerization during charge inversion mass spectrometry.

Keywords: Charge inversion mass spectrometry; DFT calculation; Dissociation mechanism; Isomeric differentiation; Chlorophenyl radical

1. Introduction

Isomers of dichlorobenzene and chlorophenol are important starting materials in the manufacture of various chemicals, such as drugs, pesticides, dyes, and thermostable polymers. These isomers are also members of the classes of compounds known as polychlorinated dibenzo-*p*-dioxines (PCDDs) and polychlorinated dibenzofurans (PCDFs), respectively, which are extremely toxic to humans and animals [1–11]. Since the toxicity of PCDDs and PCDFs depends dramatically on the chlorine substitution pattern [1–3], various mass spectrometry/mass spectrometry (MS/MS) methods enabling more rapid and sensitive structure analysis have been investigated [12–17].

Previously, we reported [18–20] that charge inversion mass spectrometry using alkali metal targets provides a means for clearly discriminating among dichlorobenzene isomers and

* Corresponding author. Tel.: +81 72 254 9714; fax: +81 72 254 9931.
E-mail addresses: hayakawa@c.s.osakafu-u.ac.jp (S. Hayakawa), matsu@c.s.osakafu-u.ac.jp (H. Matsubara), iwamoto@c.s.osakafu-u.ac.jp (K. Iwamoto).

1387-3806/$ – see front matter © 2006 Elsevier B.V. All rights reserved.
doi:10.1016/j.ijms.2006.11.017

among chlorophenol isomers. In particular, the differentiation of isomeric dichlorobenzenes, whose parent ions have similar electron ionization (EI) mass spectra and CAD spectra, was demonstrated using charge inversion mass spectrometry [18,19]. This differentiation on the basis of the dependence of the relative intensities of the $C_6H_4Cl^-$ ions to Cl^- ions upon the isomeric $C_6H_4Cl_2^+$ precursors in the charge inversion spectra was possible due to the dissociation of energy-selected neutrals formed by near-resonant neutralization with alkali metal targets [19,21–23]. The fragmentation of the excited $C_6H_4Cl_2$ in the charge inversion process provided the equal abundance of the C_6H_4Cl and Cl fragments regardless of the isomeric precursors, because the C_6H_4Cl and the Cl in the fragmentation of the excited $C_6H_4Cl_2$ formed by near-resonant neutralization are the complementary fragments and would be expected to be equal for each of the isomeric precursors. Therefore, although in our previous work we were able to demonstrate a clear difference in the charge inversion spectra among the isomeric dichlorobenzenes [18], at that time we were unable to explain satisfactorily the reason for these spectral differences.

A number of studies have been reported by others in which differentiation among the isomers of dichlorobenzene has been attempted on the basis of spectroscopic features. The dissociation of dichlorobenzenes was investigated by Ichimura et al. [24] and Zhu et al. [25] by using photo-fragmentation methods. Photoelectron spectra and penning ionization electron spectroscopy of dichlorobenzenes were reported by Ruscic et al. [26] and Fujisawa et al. [27] respectively. Threshold collision-induced dissociation for *o*- and *p*-dichlorobenzene cations was also reported by Armentrout and co-workers [28]. Although small differences between isomeric dichlorobenzenes were reported in these studies, these techniques cannot be used for rapid analysis. Previous theoretical studies on dichlorobenzenes include calculation of orbital correlation and orbital energies [26], ionization energies [29], energy and vibrational frequency of dichlorobenzene cations [28], and homolytic C–Cl bond energies in polychlorobenzenes [30].

The elucidation of the existence and/or structure of neutral radicals is difficult due to their high reactivity. The existence and/or structure of neutral radicals in the gas phase has been investigated by using neutralization re-ionization (NR) mass spectrometry [31–42]. In particular, Schwarz and co-workers have reported various radicals and neutrals by using NR, charge reversal (CR), and neutral and ion decomposition difference (NIDD) mass spectrometry, where the spectra of the radicals were obtained by subtracting normalized ion intensities in NR mass spectra from those in CR mass spectra [40,43–45]. Previously [46–48], we investigated the structure and dissociation processes of hydrocarbon radicals by using charge inversion mass spectrometry with alkali metal targets.

The aim of the present work was to provide an explanation for our previously reported differentiation among dichlorobenzene isomeric achieved using charge inversion mass spectrometry. Evidence for the existence of isomeric chlorophenyl radicals is presented on the basis of the normalized intensities in the charge inversion mass spectrometer, and computational chemistry for the relevant isomeric neutrals and radicals.

2. Materials and methods

2.1. Spectral measurements

In the charge-inversion mass spectrometer, mass-selected positive ions are made to collide with alkali metal targets, and the resulting negative ions formed upon two-electron transfer are mass-analyzed [23,49]. Sample gas was supplied into the ion source via a capillary having low gas-conductance from a heated gas inlet system (Hitachi M-8087) with a gas reservoir of 300 mL. Positive precursor ions are formed by electron ionization in the ion source and are accelerated to a kinetic energy of 3 keV. The precursor ions are mass-separated by a double focusing mass spectrometer (MS-I, Hitachi M80B). The central radius of the electric sectors is 216 mm, and the magnetic field has a 200 mm ion orbital radius. The mass-separated precursor ions enter a 3.7 cm long target chamber which is located at the exit of MS-I. The alkali metal target is supplied as vapor from a reservoir through a ball valve. The supply of the alkali metals can be turned off by closing the ball valve. The target chamber, the ball valve and the reservoir are thermally controlled in order to control the alkali metal density in the target chamber. Neutralization, dissociation and anionization take place in the target chamber filled with alkali metal vapor. The negative ions are mass-analyzed by a toroidal electrostatic analyzer (ESA), MS-II, having a 216 mm central radius. The mass-analyzed negative ions are detected by a 10 kV post-acceleration secondary electron multiplier (Hamamatsu R596).

Most of the negative ion peaks in the charge inversion spectra disappear when the supply of alkali metal vapor from the reservoir is prevented by closing the ball valve, indicating that negative ions are generated by the collision of the positive ions with alkali metal targets. Primary ion spectra, in which the target vapors were not supplied, and CAD spectra were measured by mass-analyzing the positive ions exiting the target chamber. By changing the polarity of MS-II and the multiplier, the positive ions were mass-analyzed by MS-II, and the mass-analyzed secondary ions were detected by the 10 kV post-acceleration secondary electron multiplier.

Multiplier voltages of the secondary electron multiplier of 800, 1400 and 2000 V were used to measure the primary ion spectra, the CAD spectra and the charge inversion spectra, respectively, in order to produce spectra having appropriate peak intensities. The ratio of amplification in this work was approximately 1:100:2000 at the multiplier voltages 800 V:1400 V:2000 V, respectively. The difference of the detection efficiencies between positive ions and negative ions were not obtained, because the conversion yield by the 10 keV post-acceleration depended on the polarity of the detected ions.

Ortho-, *meta*-, and *para*-dichlorobenzene (98%, Wako, Japan), $C_6H_4Cl_2$, were used as received. The decrease in primary ion peak intensity is less than 1% in 10 min measurement when using the gas inlet system with a 300 mL reservoir. Since this decrease in the sample gas over the time taken to change polarity for measuring the spectra [20], the intensities of the primary ion peaks were assumed to be identical for the measurements of

primary ion spectra, CAD spectra, and charge inversion spectra for a given dichlorobenzene sample gas.

2.2. Computational methods

Ab initio and density functional theory (DFT) calculation using the Gaussian 98 and Gaussian 03 program [50] was performed using DACS XJ-3000 and TX7/i9510 Itanium 2 computers.

Geometry optimizations were performed using standard gradient techniques at the SCF, BHandHLYP, and B3LYP levels of theory, using restricted (RHF, RBHandHLYP, and RB3LYP) and unrestricted (UHF, UBHandHLYP, and UB3LYP) methods for closed- and open-shell systems, respectively [51]. All ground and transition states were verified by vibrational frequency analysis. Further single-point calculations including QCISD and CCSD(T) methods were performed on the B3LYP and BHandHLYP optimized geometries. When correlated methods were used, calculations were carried out using the frozen core approximation. Values of $\langle s^2 \rangle$ never exceeded 0.79 before annihilation of quartet contamination at the DFT calculations. As zero-point vibrational energies and thermal enthalpies were calculated in a harmonic approximation, zero-point corrected energies and the enthalpies at 298 K were also calculated. Excitation energies were calculated with time-depended (TD) DFT method within the Gaussian 98 program.

3. Results and discussion

3.1. Reaction mechanism and normalized ion intensity

In charge inversion mass spectrometry using alkali metal targets, the fragment negative ions formed from the corresponding positive ions by transfer of two electrons are overwhelmingly more abundant than non-dissociated negative ions, which were formed via double electron transfer in single collision [52–57]. On the basis of the target density dependence of product negative ion intensity [52–55] and thermochemical considerations of the internal energy distributions [21–23], it has been demonstrated that the formation process of fragment negative ion in the charge inversion mass spectrometer occurs via near-resonant neutralization, followed by spontaneous dissociation of the excited neutrals, and then endothermic negative ion formation, as shown in the reactions in Scheme 1 [23]:

If the cross-sections for the neutralization process (reaction (1)) and the negative ion formation (reaction (3)) are expressed as σ_{neut} and σ_{nega}, respectively, then the relative intensity of product negative ions from primary positive ions I_{nega}/I_{posi} in the charge inversion reactions in Scheme 1 is given by the following

$$AB^+ + T \rightarrow AB^* + T^+ \quad (1)$$
$$AB^* \rightarrow A + B \quad (2)$$
$$B + T \rightarrow B^- + T^+ \quad (3)$$

Scheme 1.

equation [19]:

$$\frac{I_{nega}}{I_{posi}} = \frac{\sigma_{neut}\ \mathrm{BR}\ \sigma_{nega} D^2 l^2}{2} \quad (4)$$

where BR is the branching ratio resulting in the formation of A + B in reaction (2) competing with other dissociation channels. The intensities of the secondary negative ions at the exit and positive precursor ions at the entrance of the target chamber are I_{nega} and I_{posi}, respectively. D is the target density, and l is the target length. The target length l of our charge inversion mass spectrometer is constant in the present work. When the target density is constant, the relative negative ion intensity I_{nega}/I_{posi} provides information about the product $\sigma_{neut}\,\mathrm{BR}\,\sigma_{nega}$. In order to compare $\sigma_{neut}\,\mathrm{BR}\,\sigma_{nega}$ among isomeric precursors, the normalized negative ion intensities Norm (I_{nega}/I_{posi}), which are proportional to the relative negative ion intensities I_{nega}/I_{posi}, are evaluated by using the charge inversion spectra and the primary ion spectra.

The CAD process proceeds via excitation of ions followed by their dissociation, as shown in the reactions in Scheme 2:

$$AB^+ + T \rightarrow AB^{+*} + T \quad (5)$$
$$AB^{+*} \rightarrow A^+ + B \quad (6)$$

Scheme 2.

If the cross-section of excitations in reaction (5) are expressed as σ_{ext}, the relative intensity of the fragment positive ions from the primary positive ions I_{fra}/I_{posi} in the CAD reactions shown in Scheme 2 is given by the following equation [19]:

$$\frac{I_{fra}}{I_{posi}} = \sigma_{ext}\ \mathrm{DR}\ Dl \quad (7)$$

where DR is the ratio of dissociation that yields A^+ in reaction (6). The intensities of positive fragment ions at the exit and positive precursor ions at the entrance of the target chamber are I_{fra} and I_{posi}, respectively. The relative fragment ion intensity I_{fra}/I_{posi} provides information about the product $\sigma_{ext}\,\mathrm{DR_a}$. In order to compare $\sigma_{ext}\,\mathrm{DR_a}$ among isomeric precursors, the normalized fragment ion intensities Norm (I_{fra}/I_{posi}), which are proportional to the relative fragment ion intensities I_{fra}/I_{posi}, are evaluated by using the CAD spectra and the primary ion spectra.

The normalized negative ion intensity Norm (I_{nega}/I_{posi}) in the charge inversion spectra, and the normalized positive ion intensity Norm (I_{fra}/I_{posi}) in the CAD spectra, can be compared among the isomeric dichlorobenzenes by adjusting the multiplier voltage to amplify the ion peak intensities in the respective primary, CAD, and charge inversion spectra to provide a constant amplification. Since it was difficult to make the peak intensities of the different isomeric $C_6H_4Cl_2^+$ precursor ions the same, the normalized charge inversion spectra were obtained by dividing the charge inversion spectra by the intensities of the primary ions in the relevant primary ion spectra, where the negative ion intensities were also divided by the ratio of the amplification depending on the multiplier voltage. Similarly, the normalized CAD spectra were obtained by dividing the CAD spectra by the intensities of the primary ions in the relevant primary ion spectra. The

conversion yield in the 10 keV post-acceleration and the transmission factors in the ESA may provide different ratios between the primary ions and both positive and negative fragment ions. By these different ratios, the ion intensities between the negative ions in the normalized charge inversion spectra and the fragment positive ions in the normalized CAD spectra cannot be directly compared. However, when comparing the fragment ions of the same mass, both the relative negative ion intensities I_{nega}/I_{posi} and relative fragment ion intensities I_{fra}/I_{posi} are proportion to the normalized intensity. The target density was kept almost constant during the several minutes required for the measurement of the spectra of primary positive ions, CAD, and charge inversion, by maintaining the target heating system at a constant the temperature [20]. Using this normalization procedure, the product σ_{neut} BR σ_{nega} in the charge inversion processes and the product σ_{ext} DR in the CAD processes can be compared among the isomeric $C_6H_4Cl_2^+$ precursors, from the normalized negative ion intensities Norm (I_{nega}/I_{posi}) in the charge inversion spectra and from the normalized positive ion intensities Norm (I_{fra}/I_{posi}) in the CAD spectra, respectively.

3.2. CAD spectra

Fig. 1 shows the primary ion spectra and the CAD spectra obtained using a Cs target for $C_6H_4{}^{35}Cl_2^+$ ions obtained from *o*-, *m*-, and *p*-$C_6H_4Cl_2$ by electron ionization (EI). The $C_6H_4{}^{35}Cl_2^+$ ions of $m/z = 146$, which give rise to the strongest peak in the EI spectra, were selected as precursor ions for all of the spectra in Fig. 1. In the primary ion spectra shown in Fig. 1a–c, the peaks associated with $C_6H_4{}^{35}Cl_2^+$ ions at $m/z = 146$ are the only ones observed because the ball valve was closed, thereby preventing supply of the target gas. The intensity ratios of the peaks of the precursors *o*-, *m*-, and *p*-$C_6H_4{}^{35}Cl_2^+$ ions of $m/z = 146$ in Fig. 1a–c are 1.00:0.70:0.78, respectively. Since a constant electron impact current of 100 μA, and a constant electron impact energy of 70 eV were used in the measurement of each spectra, the differences in the peak intensities observed in Fig. 1a–c are mainly due to variations in the primary gas density in the ion source.

The CAD spectra shown in Fig. 1d–f were measured under the same conditions as the spectra in Fig. 1a–c, respectively, except for the presence of the target gas and adjustment of the multiplier voltage. In the CAD spectra shown in Fig. 1d–f, the peak intensities of the non-dissociated $C_6H_4{}^{35}Cl_2^+$ ions at $m/z = 146$ are much lager than the ordinate scale in the figures, and apparently look more intense than those in corresponding spectra in Fig. 1a–c due to the different multiplier voltage used for the CAD spectra. The actual ion intensities of the non-dissociated ions in Fig. 1d–f are weaker than those in the respective primary ion spectra in Fig. 1a–c due to neutralization and scattering by the alkali metal targets. In each of these CAD spectra, the peaks associated with $C_6H_4Cl^+$ ($m/z = 111$) ions resulting from loss of a Cl atom are the most dominant fragment peaks. The peaks at $m/z = 75$ are associated with $C_6H_3^+$ ions resulting from loss of one H atom and two Cl atoms. The profiles of the peaks arising from dissociation of the precursor ions are similar for

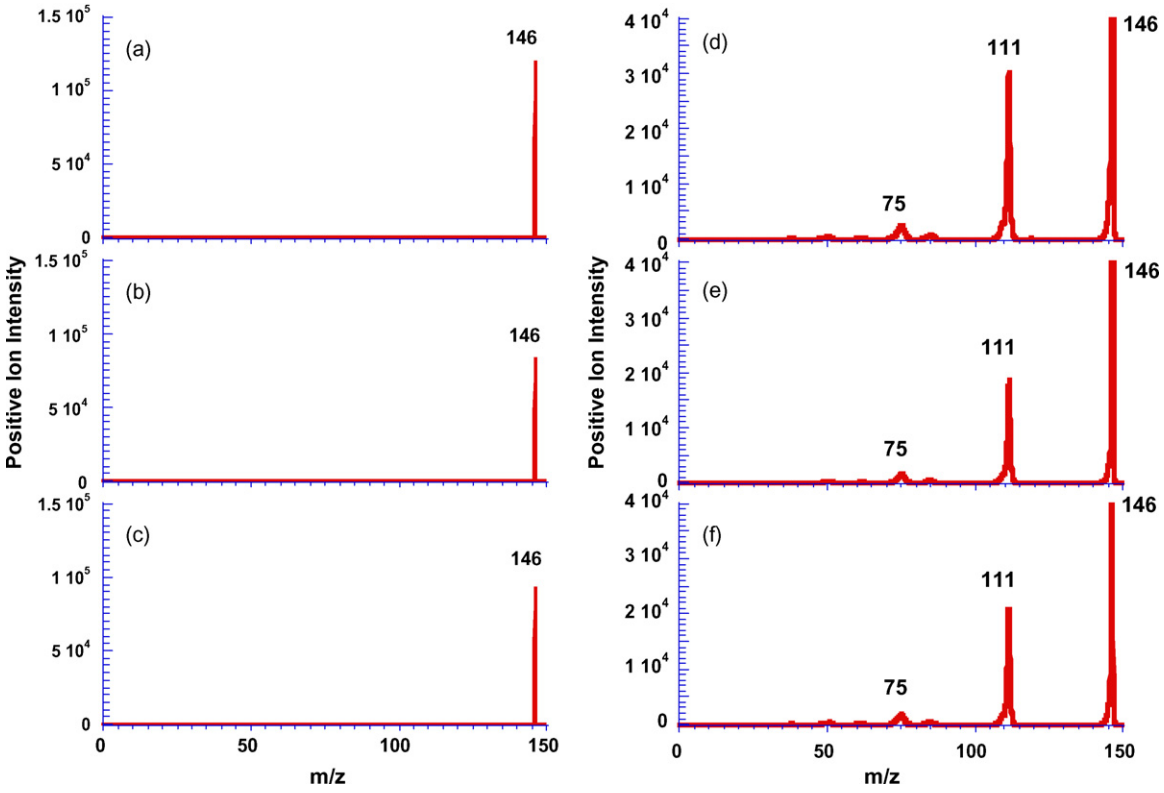

Fig. 1. Primary ion spectra for the $C_6H_4Cl_2^+$ ions of *o*-, *m*-, and *p*-dichlorobenzene, denoted by (a), (b), and (c), respectively, and collisionally activated dissociation (CAD) spectra of $C_6H_4Cl_2^+$ ions of *o*-, *m*-, and *p*-dichlorobenzene, denoted by (d), (e), and (f), respectively. In the primary ion spectra, target gas was not supplied from the reservoir. Multiplier voltages of the electron multiplier were 800 V for the primary spectra and 1400 V for the CAD spectra.

each of the structural isomers. The intensity ratios of the peaks at $m/z = 111$ in the CAD spectra of *o*-, *m*-, and *p*-$C_6H_4{}^{35}Cl_2{}^+$ ions are 1.00:0.61:0.69, respectively, and are similar to those for the peaks at $m/z = 146$ in the corresponding primary ion spectra. This similarity in the intensity ratios for the primary ion spectra and the CAD spectra of the isomeric dichlorobenzenes indicates that the intensity differences in the CAD spectra are determined mainly by the precursor ion intensities.

In order to compare the normalized positive ion intensities and the products σ_{ext} DR in the CAD spectra among the isomeric dichlorobenzenes, compensation for the differences in the primary ion intensity is necessary. This normalization was achieved by dividing the peak intensities in the CAD spectra (and the charge inversion spectra) according to the relevant primary ion intensity for the *ortho*-, *meta*-, and *para*-isomers, respectively. These normalized spectra, in which the difference of the amplification by the multiplier voltage is counted, are shown in Fig. 2. After normalization, the peak intensities associated with $C_6H_4Cl^+$ ($m/z = 111$) ions in the CAD spectra for each the isomeric dichlorobenzenes are similar, as shown in Fig. 2a–c. The intensity ratios for the peak associated with $C_6H_4Cl^+$ ($m/z = 111$) ions in the normalized CAD spectra are 1.0:0.87:0.88, for *o*-, *m*-, and *p*-dichlorobenzenes, respectively. This similarity in the normalized peak intensity for the $C_6H_4Cl^+$ ion ($m/z = 111$) of each of the isomeric precursor indicates that the values for the product, σ_{ext} DR, are practically the same for each isomeric precursors, since the experimental conditions associated with the target results in a constant value for the product, *Dl*. While the excitation cross-sections, σ_{ext}, and the dissociation rate, DR, generally depend on internal energy, the internal energy distributions are assumed to be the same as the internal energy distributions of high-energy CAD reported for thermometer molecules such as tungsten hexacarbonyl [21,58].

Little difference in the dissociation of the isomeric ions of *ortho*- and *para*-dichlorobenzene was reported in the threshold energy region by Armentrout and co-workers [28]. The similarity of the CAD spectra of the isomeric precursors in the high-energy region observed in the present work is consistent with the results reported by Armentrout and co-workers. At the same time, the similarity of the normalized fragment on intensities Norm (I_{fra}/I_{posi}) among the isomeric dichlorobenzenes in the normalized CAD spectra indicates that the dissociation process for the isomeric $C_6H_4Cl_2{}^+$ ions activated by the high-energy collision are similar for the *o*-, *m*-, and *p*-dichlorobenzenes.

3.3. Charge inversion spectra

The intensities of the peak associated with Cl^- ions ($m/z = 35$) in the normalized charge inversion spectra for the isomeric precursor ions using a Cs target are almost same, as shown in Fig. 2d–f, where the intensity ratios for the peak associated with Cl^- ions from *o*-, *m*-, and *p*-dichlorobenzenes are

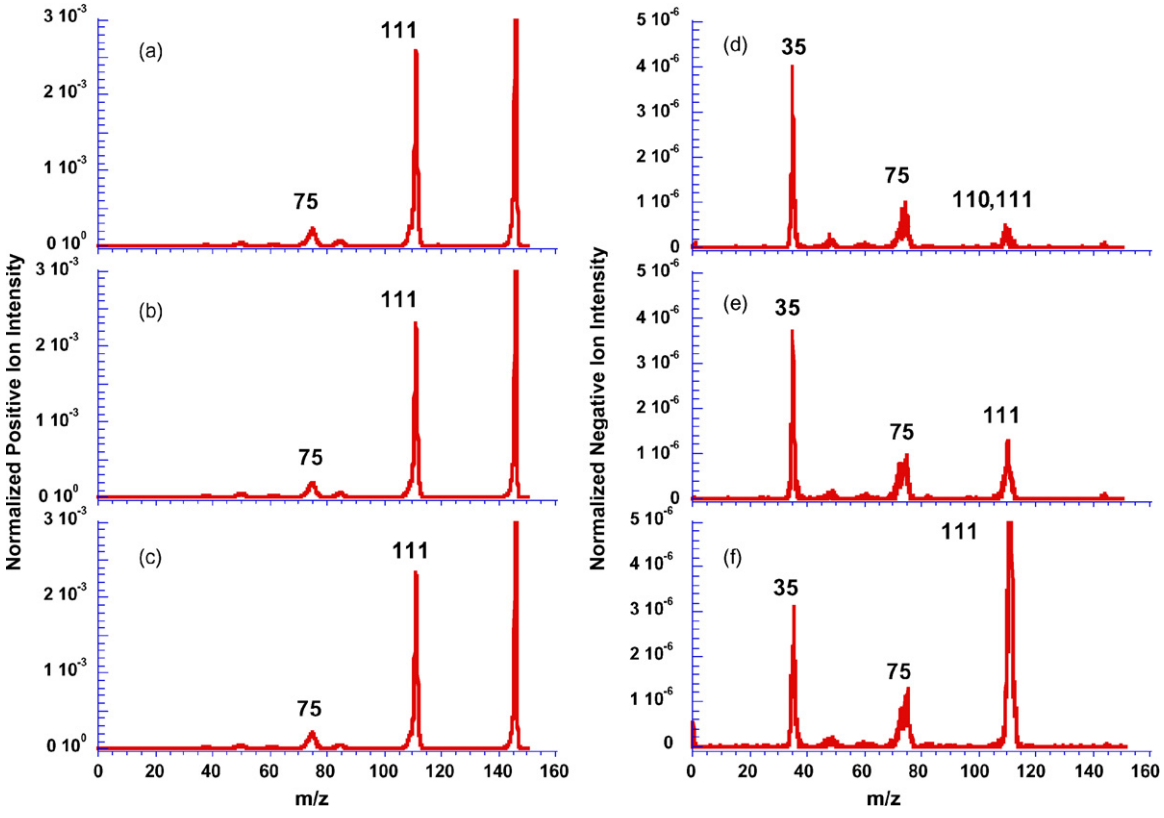

Fig. 2. Normalized CAD spectra of $C_6H_4Cl_2{}^+$ ions of *o*-, *m*-, and *p*-dichlorobenzene denoted by (a), (b), and (c), respectively, and normalized charge inversion spectra of $C_6H_4Cl_2{}^+$ ions of *o*-, *m*-, and *p*-dichlorobenzene denoted by (d), (e), and (f), respectively. The target was Cs and the collision energy was 3.0 keV. The ordinates were normalized by the intensity of the respective primary ions shown in Fig. 1. Multiplier voltages of the electron multiplier were 1400 V for the CAD spectra and 2000 V for the charge inversion spectra.

1.00:1.08:1.06, respectively. On the other hand, the intensity of the peak associated with $C_6H_4Cl^-$ ions ($m/z = 111$) in the *meta*-isomer is much larger than that for the *ortho*-isomer, as shown in Fig. 2d and e, and the intensity of this peak for the *para*-isomer spectrum was so high that it is off scale on the ordinate range used in Fig. 2f. The small difference in the intensity of the Cl^- ions for the normalized spectra of the isomeric precursors shown in Fig. 2d–f indicates that the magnitude of the product σ_{neut} BR σ_{nega} for Cl^- ion formation must be almost identical for each of the isomeric precursors because, as for the normalized CAD spectra, the experimental conditions of the target in the charge inversion spectra result in a constant value for the product D^2l^2. Since σ_{nega} for Cl^- ion formation is identical for any of isomeric precursor, the similar value of the product σ_{neut} BR σ_{nega} for Cl^- ion formation indicates that the magnitude of the product σ_{neut} BR regarding the reactions (1) and (2) in Scheme 1 are assumed to be the same among the isomeric dichlorobenzenes.

The normalized charge inversion spectra using Cs and K targets are shown in Fig. 3. The ion intensities in the normalized charge inversion spectra between the Cs target in Fig. 3a–c and the K target in Fig. 3d–f cannot be directly compared because of the different target density D between for the Cs the K target. Similarly in the case of the Cs target, the normalized peak intensities associated with the Cl^- ions ($m/z = 35$) using the K target are almost same, as shown in Fig. 3d–f, where the intensity ratios for the peak associated with Cl^- ions from *o*-, *m*-, and *p*-dichlorobenzenes are 1.00:0.83:1.07, respectively. Near unit value of the ratio of the peak intensity of Cl^- ions for both the Cs and K target indicated that the magnitude of the product σ_{neut} BR σ_{nega} for the reactions of Cl^- ion formation in Scheme 1 are the same among the isomeric dichlorobenzenes.

On the other hand, the intensity of the peak associated with $C_6H_4Cl^-$ ions ($m/z = 111$) showed strong dependence on the isomeric precursors, both for the Cs target, as shown in Fig. 3a–c, and for the K target, as shown in Fig. 3d–e. The intensity ratios for the peak associated with $C_6H_4Cl^-$ ($m/z = 111$) ions in the charge inversion spectra of the *ortho*-, *meta*-, and *para*-isomers using the Cs target were 1.0:2.5:16.9, respectively. The intensity ratios for the K target are 1.0:1.9:11.4 for *o*-, *m*-, and *p*-isomers. The clear discrimination among *o*-, *m*-, and *p*-dichlorobenzene isomers using the charge inversion spectrometry is attributed to the difference in the normalized negative intensities Norm (I_{nega}/I_{posi}) for the isomeric $C_6H_4Cl^-$ ions. The relative abundance of Cl^- ions is essentially independent of isomeric precursor, whereas the relative abundance of the isomeric $C_6H_4Cl^-$ ions displays a strong isomeric dependence. As seen from reactions (1) and (2) in Scheme 1, the magnitude of the product σ_{neut} BR for Cl and C_6H_4Cl are assumed to be the same because Cl and C_6H_4Cl are complementary fragments. As a result of this, the difference in the intensities observed in Fig. 3 for the peaks associated with $C_6H_4Cl^-$ ions derived from the isomeric precursors must be attributed to the differences in the magnitude of the cross-section for negative ion formation from

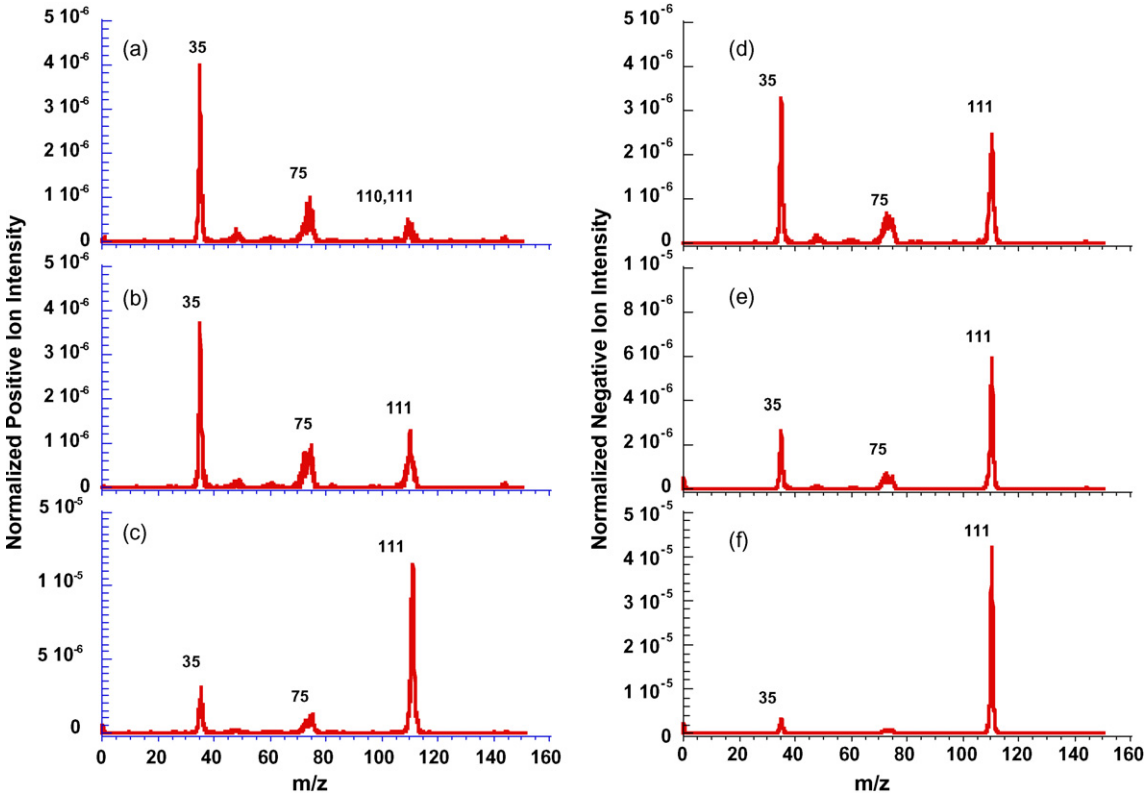

Fig. 3. Normalized charge inversion spectra of $C_6H_4Cl_2^+$ ions of *o*-, *m*-, and *p*-dichlorobenzene using a Cs target, are denoted by (a), (b), and (c), respectively, and the spectra of $C_6H_4Cl_2^+$ ions of *o*-, *m*-, and *p*-dichlorobenzene using a K target, denoted by (d), (e) and (f), respectively. The intensities of the peaks associated with $C_6H_4Cl^-$ in the charge inversion spectra show a strong dependence on the isomeric structures for both Cs and K targets, whereas those associated with Cl^- ions are almost same for each isomer.

the isomeric chlorophenyl radicals, σ_{nega}. Furthermore, the differences in the intensities of the peaks at $m/z = 111$ implies that isomerization among the isomeric chlorophenyl radicals does not occur in the charge inversion mass spectrometer.

Another possibility for the isomeric differentiation is the formation of benzyne and Cl_2 in dissociation reaction (2) in Scheme 1. This dissociation process is inferred to depend on the isomeric structure due to the fact that the *ortho*-isomer readily decomposes to benzyne and Cl_2. The electron affinities of *o*- and *p*-benzyne evaluated by the photoelectron spectra of the anions were 0.564 ± 0.007 and 1.265 ± 0.008 eV, respectively, [59] and the reliable value of the electron affinity of Cl_2 is 2.4 ± 0.2 eV [60]. If these fragments are formed in Scheme 1, these negative ions are expected to be detected in the charge inversion spectra especially in *ortho*-isomers, as both benzyne and Cl_2 have positive electron affinities. From the fact that the peaks at $m/z = 70$ and 76 are not observed in any of the charge inversion spectra, as shown in Fig. 3, it was concluded that the dissociation into benzyne and Cl_2 is not involved in the charge inversion process in Scheme 1.

3.4. Calculated geometries, bond energies and electron affinities

Geometry optimization of *o*-, *m*-, and *p*-dichlorobenzenes (**1a**–**3a**), *o*-, *m*-, and *p*-chlorophenyl radicals (**1b**–**3b**), and *o*-, *m*-, and *p*-chlorophenyl anions (**1c**–**3c**) was carried out at the B3LYP/6-31 + G(d,p) level of theory. In addition, the *ortho*-isomers (**1a**–**1c**) were also optimized at the HF/6-31G(d), HF/6-31 + G(d,p), HF/6-311 + G(d,p), BHandHLYP/6-31G(d), BHandHLYP/6-31 + G(d,p), and B3LYP/6-31G(d) levels of theory. The important geometric features of isomeric dichlorobenzenes, **1a**–**3a**, the radicals, **1b**–**3b**, and the anions, **1c**–**3c**, at the B3LYP/6-31 + G(d,p) level are summarized in Fig. 4. Calculated bond dissociation energies (E_{BD}) of the C–Cl bond in *ortho*-dichlorobenzenes, and electron affinities (E_{EA}) of the *ortho*-isomeric radicals are listed in Table 1, while the E_{BD} values for the C–Cl bond in each of the isomeric chlorobenzenes, and the E_{EA} of the isomeric radicals, calculated at the B3LYP/6-311 + G(2df,p)//B3LYP/6-31 + G(d,p) level of theory are listed in Table 2.

Inspection of Fig. 4 reveals that while the bond length of C–Cl in the *o*-dichlorobenzene molecule, **1a**, and its corresponding radical, **1b**, are predicted to be almost the same, at around 1.75 Å, this bond length in the anion, **1c**, is predicted to be longer, at around 1.90 Å. In addition, the bond angle (α) at the carbon where the attached chlorine is lost in **1a** and **1b** is predicted to be in the range 120–125°, whereas that in **1c** is calculated to be significantly smaller, at around 112°. In conclusion, while the structures of the radicals, **1b**–**3b**, are predicted to be very similar to those of dichlorobenzenes, **1a**–**3a**, the geometries of the anions, **1c**–**3c**, are predicted to be distorted at all levels of theory.

Inspection of Table 1 reveals that the bond dissociation energies (E_{BD}) are calculated to be 2.323 eV at the HF/6-31G(d) level of theory. Improvements in basis set quality appear to have little effect on this number. However, as expected, electron correlation is important in this calculation; DFT calculations serve to raise this energy to 3.769 eV (BHandHLYP/6-31G(d)) and 3.927 eV (B3LYP/6-31G(d)). Inclusion of zero-point vibrational energy correlation (ZPE) decreases these energies by about 0.1 eV. At the highest level of theory employed (CCSD(T)/6-31 + G(d,p)//BHandHLYP/6-31 + G(d,p)), a E_{BD} value of 4.010 eV is predicted for the

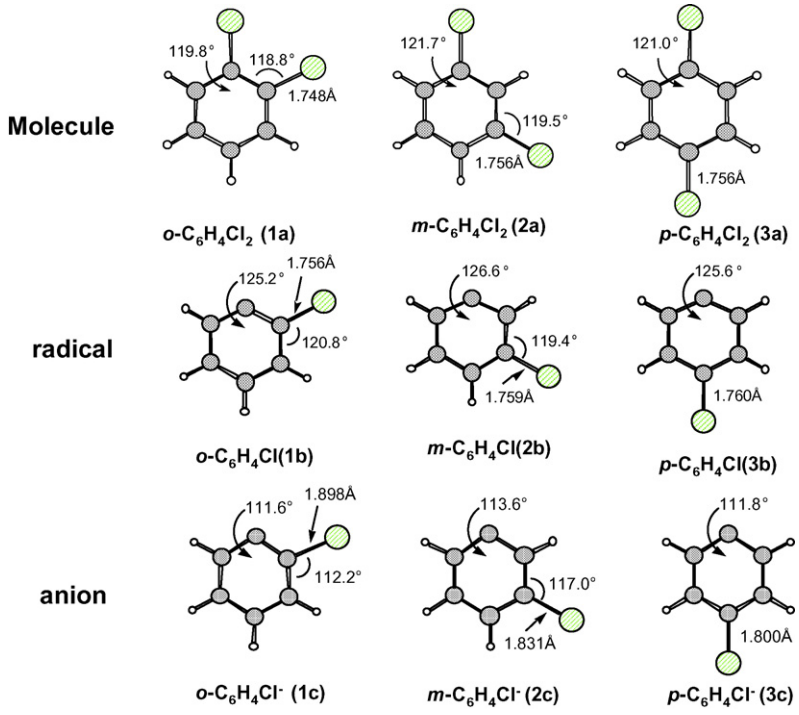

Fig. 4. B3LYP/6-31 + G(d,p) optimized geometries of *ortho*-, *meta*-, and *para*-dichlorobenzenes, and their corresponding radicals and anions.

Table 1
Calculated bond dissociation energies (E_{BD}) of the C–Cl bond in *o*-dichlorobenzene (**1a**), electron affinities (E_{EA}) of *o*-chlorophenyl radical (**1b**), and their enthalpy differences at 298 K (ΔH_{BD} and ΔH_{RE}), in eV

Method	E_{BD}	E_{BD} + ZPE	ΔH_{BD}	E_{EA}	E_{EA} + ZPE	ΔH_{EA}
HF/6-31G(d)	2.323	2.162	2.202	−0.458	−0.459	−0.457
HF/6-31 + G(d,p)	2.308	2.150	2.190	0.042	0.036	0.039
HF/6-311 + G(d,p)	2.338	2.179	2.219	0.080	0.075	0.077
BHandHLYP/6-31G(d)	3.769	3.672	3.706	0.880	0.940	0.935
BHandHLYP/6-31 + G(d,p)	3.716	3.617	3.651	1.415	1.466	1.462
BHandHLYP/6-311 + G(2df,p)//BHandHLYP/6-31 + G(d,p)	3.817	–	–	1.398	–	–
BHandHLYP/aug-cc-pVDZ//BHandHLYP/6-31 + G(d,p)	3.733	–	–	1.469	–	–
B3LYP/6-31G(d)	3.927	3.833	3.866	1.145	1.210	1.199
B3LYP/6-31 + G(d,p)	3.858	3.763	3.796	1.713	1.768	1.762
B3LYP/6-311 + G(2df,p)//B3LYP/6-31 + G(d,p)	3.951	–	–	1.694	–	–
B3LYP/aug-cc-pVDZ//B3LYP/6-31 + G(d,p)	3.890	–	–	1.757	–	–
QCISD/6-31 + G(d,p)//BHandHLYP/6-31 + G(d,p)	3.930	–	–	1.618	–	–
CCSD(T)/6-31 + G(d,p)//BHandHLYP/6-31 + G(d,p)	4.010	–	–	1.678	–	–

C–Cl bond dissociation energy of *o*-dichlorobenzene (**1a**). It is interesting to compare this value with that calculated using the B3LYP single-point calculations, which provides values of 3.951 eV (B3LYP/6-311 + G(2df,p)//B3LYP/6-31 + G(d,p)) and 3.958 eV (B3LYP/aug-cc-pVDZ//B3LYP/6-31 + G(d,p)), while the BHandHLYP calculations serve to lower the energies by about 0.1 eV.

Table 1 also provides some interesting trends in electron affinities (E_{EA}). As expected, inclusion of diffuse functions to the bases set employed is very important, which lowers the energies by about 0.50 eV. At the highest level of theory used (CCSD(T)/6-31 + G(d,p)//BHandHLYP/6-31 + G(d,p)), a E_{EA} value of 1.678 eV is calculated for the electron affinity of *o*-chlorophenyl radical (**1b**). As shown in the tables, the E_{EA} values provided by B3LYP calculations with diffuse functions are close to this value, while the BHandHLYP methods serve to raise the energies by about 0.3 eV. The data provided in Table 1 reveal that the B3LYP calculations predict E_{BD} and E_{EA} values that are comparable to those at the CCSD(T)/6-31 + G(d,p)//BHandHLYP/6-31 + G(d,p) level, providing a useful benchmark and confidence in the performance of the B3LYP method in this study, whose values for all isomers are shown in Table 2.

Inspection of Table 2 reveals that while bond dissociation energies (E_{BD}) for the *meta*- and *para*-isomers, **2a** and **3a**, respectively, are calculated to be almost the same as the values for the *ortho*-isomer **1a**, the electron affinities (E_{EA}) for both molecules **2b** and **3b** are lower than for the *o*-isomer **1b** by about 0.3 eV.

Table 2
B3LYP/6-311 + G(2df,p)//B3LYP/6-31 + G(d,p) calculated dissociation energies (E_{BD}) of the C–Cl bond of the isomeric dichlorobenzenes, and electron affinities (E_{EA}) of the isomeric radicals, in eV

	ortho	*meta*	*para*
Bond energy of C–Cl	3.951 (**1a**)	3.992 (**2a**)	4.023 (**3a**)
Adiabatic electron affinity	1.694 (**1b**)	1.442 (**2b**)	1.370 (**3b**)
Vertical electron affinity	1.315	1.117	1.021

The lowest excitation energies for singlet and triplet excited states of *o*-, *m*-, and *p*-dichlorobenzenes calculated at the TD-B3LYP/6-311 + G(2df,p)//B3LYP/6-31 + G(d,p) level of theory are listed in Table 3 [61]. As expected, the excitation energies for the triplet states of all dichlorobenzenes (**1a**–**3a**) are predicted to be smaller than those for the singlet states. Table 3 also shows that the excitation energies for all isomers of dichlorobenzene are calculated to be very similar to one another.

3.5. Thermochemical analysis of the charge inversion process

The heats of formation of *o*-, *m*-, and *p*-dichlorobenzenes obtained experimentally are 0.342, 0.291, and 0.255 eV, respectively [60]. Although the bond dissociation energies of C–Cl in dichlorobenzenes (E_{BD}) for each of the isomers have not been reported experimentally, the value of E_{BD} of C–Cl is assumed to be almost the same as that reported for chlorobenzene (4.2 eV) [24,30,60,62]. As shown in Tables 1 and 2, the calculated bond dissociation energies obtained in this study are in reasonable agreement with this value of E_{BD} obtained from experiment. In addition, the data in these Tables show that the enthalpy differences (ΔH_{BD} and ΔH_{EA}) for the bond dissociations and the electron affinities for the molecules in this study are calculated to be very similar to the calculated electronic energies.

The energy level diagram shown in Fig. 5 was constructed on the basis of this information, where the energy levels of fragments are estimated from the calculated [60] bond energy and the heats of formation of the respective dichlorobenzene, and the ionization potentials [60] of potassium and cesium. The

Table 3
TD-B3LYP/6-311 + G(2df,p)//B3LYP/6-31 + G(d,p) calculated excitation energies for the lowest singlet and triplet excited states of the isomeric dichlorobenzenes, in eV

	ortho	*meta*	*para*
Triplet	3.560	3.563	3.526
Singlet	4.839	4.863	4.890

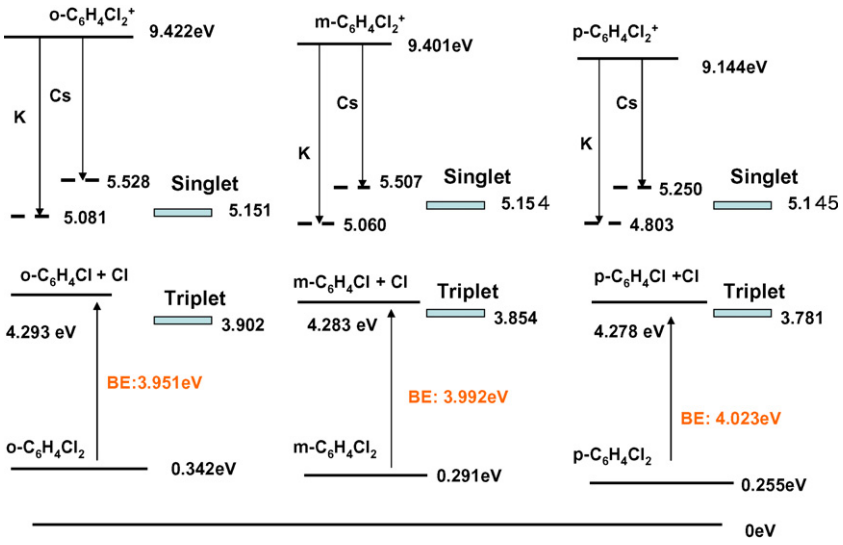

Fig. 5. Heats of formation of *o*-, *m*-, and *p*-dichlorobenzene and the parent ions, in eV. The thermochemical data are taken from Ref. [60]. The values shown next to the dotted lines are the energy values predicted for near-resonant neutralization. The energy levels for *o*-, *m*-, *p*-$C_6H_4Cl + Cl$ were evaluated from the C–Cl bond energies of the respective dichlorobenzenes shown in Table 1. The levels of the excited singlet and doublet states were evaluated from the excitation energies of the respective dichlorobenzenes shown in Table 3.

energy levels of the lowest singlet and triplet excited states of dichlorobenzenes were estimated in the same way by adding the respective heats of formation of the isomeric dichlorobenzene neutrals to the calculated excitation energies listed in Table 3, and are also shown in Fig. 5.

The levels of the fragments for *o*-, *m*-, and *p*-dichlorobenzenes of 4.293, 4.283 and 4.278 eV, respectively, were determined from the calculated C–Cl bond energies shown in Table 2, and the heats of formation of the isomeric dichlorobenzene neutrals. The differences of 0.1 eV for the fragment energy levels are much smaller than the absolute bond energy about 4 eV.

Dashed lines represent "expected energy levels" of the excited dichlorobenzene neutrals associated with near-resonant neutralization, and are lower by an amount corresponding to the ionization energy associated with cation formation of the relevant alkali metal target. It is noteworthy that the "expected energy levels" are assumed to be the same as that reported previously [21–23]. On the other hand, the excited dichlorobenzene neutrals may lie in both singlet and triplet states by the spin conservation rule. As shown in Fig. 5, the energy levels of the singlet excited states of isomeric dichlorobenzenes produced using K accord with the "expected energy levels" of the excited dichlorobenzene neutrals. Although energy levels of the triplet excited states are calculated to be lower than the "expected energy levels", higher energy levels of the triplet excited states can be formed by the near-resonance neutralization. Accordingly, the calculation result that energy levels of the singlet or triplet excited states exist close to the "expected energy levels" of the excited dichlorobenzenes strongly suggests that the neutralizations with alkali metal target would take place as near-resonance processes having large cross sections. On the other hand, the "expected energy levels" are much lower than that for successive dissociation into benzyne and two Cl atoms, since the C–Cl bond energies are estimated to be around 4 eV. Although the formation of benzyne and two Cl atoms could explain the isomeric differentiation, inspection for the energy levels in Fig. 4 rejects possibility of the successive dissociation pathway.

Photo-dissociation of dichlorobenzenes reported by Ichimura et al. [24] showed only small differences in the translational energy distribution spectra for the Cl fragments from the isomers, and the existence of isomeric $C_6H_4Cl^{\bullet}$ radicals was not discussed by these authors. The near-resonant levels of the excited neutrals of all isomers are evaluated from the heats of formation of the isomeric dichlorobenzene cations and ionization energy of the targets. The near-resonant levels for the various targets are almost the same due to the similar values for the heats of formation for the isomeric dichlorobenzene cations. Since the levels are about 1 eV higher than the energy of fragments ($C_6H_4Cl^{\bullet} + Cl^{\bullet}$), the excited $C_6H_4Cl_2^{*}$ formed from near-resonant neutralization are presumed to dissociate spontaneously into $C_6H_4Cl^{\bullet} + Cl^{\bullet}$, which would explain the absence of non-dissociated negative ions in the charge inversion spectra in Figs. 2 and 3.

3.6. Isomerization of chlorophenyl radicals

Extensive searching of the C_6H_5Cl potential energy surfaces at the B3LYP/6-31 + G(d,p) level of theory located hypervalent species **4** and **5** (see Fig. 6) as transition states in the isomerization between the *o*-chlorophenyl (**1b**) and *m*-chlorophenyl (**2b**) radicals, and the *m*-chlorophenyl (**2b**) and *p*-chlorophenyl (**3b**) radicals, respectively. Analysis of force constants associated with structures **4** and **5** reveals that they correspond to the transition states for the isomerization of the radicals. The important geometric features of the transition states and a schematic diagram of the calculated isomerization barriers are shown in Fig. 6, and the B3LYP/6-311 + G(2df,p)//B3LYP/6-31 + G(d)-calculated energy barriers ($\Delta E_1^{\ddagger}$ and $\Delta E_2^{\ddagger}$ in Scheme 3) are listed in Table 4.

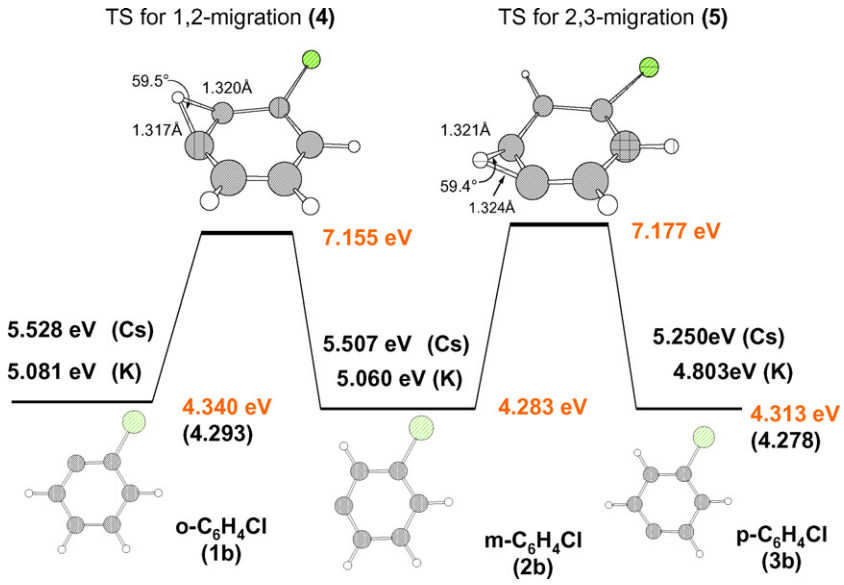

Fig. 6. Schematic diagram of isomerization barriers for *o*-, *m*-, *p*-C_6H_4Cl radicals. The isomerization barriers are much higher than the energy levels of the excited $C_6H_4Cl_2$ corresponding near-resonant state using K or Cs targets.

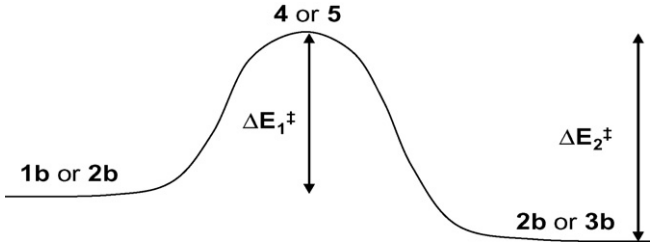

Scheme 3.

Inspection of Table 4 reveals the large energy barriers for the forward and reverse isomerization between the chlorophenyl radicals, calculated on the B3LYP/6-311 + G(2df,p)//B3LYP/6-31 + G(d,p). Interestingly, the geometries for both transition states **4** and **5** are predicted to have a hydrogen atom which is bridged between two carbon atoms and which lies out of plane of the benzene ring. Indeed, the angles between the benzene rings and the triangles formed by the 1,2- and 2,3-migrating hydrogen are calculated to be 107.7° and 104.3°, respectively. The large energy barriers of more than 2.8 eV for both the *ortho*- to *meta*-isomerization and the *meta*- to *para*-isomerization are rationalized by this deformation of the bridged hydrogen atom in the transition states.

The values of 7.155 and 7.177 eV shown in Fig. 6 are the heats of formation that correspond to the energy barriers evaluated from the *meta*-isomers calculated using the energy differences given in Table 2. These energy levels are much higher than the energies of the excited $C_6H_4Cl_2$ neutrals expected from the near-resonant neutralization with Cs of K targets, which are 5.5 and 5.0 eV, respectively. The magnitude of these barriers to isomerization means that the $C_6H_4Cl^\bullet$ fragments formed on dissociation of the excited $C_6H_4Cl_2$ neutrals are unlikely to isomerize, and this would explain the presence of the isomeric $C_6H_4Cl^\bullet$ radicals formed on dissociation of the respective dichlorobenzene isomers.

As shown in Fig. 5, the differences in the energies of the excited dichlorobenzenes and those of their fragments $C_6H_4Cl^\bullet + Cl^\bullet$ are almost identical for each of the isomeric dichlorobenzenes, and so the abundances of Cl fragments, as determined from the product σ_{neut} BR, are expected to be the same for each of the isomeric dichlorobenzenes. The abundance of Cl^- ions formed from the $Cl^\bullet$ radicals in the charge inversion spectrometer is given by Eq. (4). Therefore, the fact that the abundances of Cl^- ions in the normalized charge inversion spectra in Fig. 2a–c are almost the same can be explained by the cross-section for formation of Cl^- ions from the $Cl^\bullet$ radicals, σ_{nega}, being virtually identical for each of the isomeric precursors.

Table 4
B3LYP/6-311 + G(2df,p)//B3LYP/6-31 + G(d,p)-calculated energies barriers for the forward ($\Delta E_1^\ddagger$) and reverse ($\Delta E_2^\ddagger$) isomerization of chlorophenyl radicals, in eV

	$\Delta E_1^\ddagger$	$\Delta E_2^\ddagger$
1b–2b	2.815	2.872
2b–3b	2.894	2.864

3.7. *Effect of electron affinity on the charge inversion spectra*

Adiabatic and vertical electron affinities of *o*-, *m*-, *p*-chlorophenyl radicals calculated on the B3LYP/6-311 + G(2df,p)//B3LYP/6-31 + G(d,p) level of theory are tabulated in Table 2, and were found to all have positive values. Not unexpectedly, the vertical electron affinities of the isomers are higher than those of the respective adiabatic values [19]. As shown in Fig. 4, the C–Cl bond lengths of *o*-, *m*-, and *p*-chlorophenyl anions (**1c**–**3c**) are predicted to be 1.898, 1.831, and 1.800 Å, respectively, whereas this bond length is

calculated to have a value of around 1.76 Å for each of the *o*-, *m*-, and *p*-chlorophenyl radicals (**1b**–**3b**). Therefore, the degree of geometrical distortion in the isomeric anions formed from the corresponding radicals is in the order: *ortho* > *meta* > *para*. It is noteworthy that the magnitudes of the calculated electron affinities (E_{EA}) follow the same order as the found in the levels of geometric distortion. However, the differences in the adiabatic and vertical electron affinities between the isomeric chlorophenyl radicals are small.

Estimation of the cross-sections for electron transfer, other than those associated with atomic collisions using alkali metal targets, is difficult [63]. In the charge inversion spectra, the time-scale for collision-induced negative ion formation is 10^{-16} s, which is much shorter than the vibrational frequency time, so the Franck–Condon transition determines the cross-section. Therefore, it is expected that the cross-section for negative ions formation from neutrals is likely to depend on the vertical electron affinities. In the charge inversion spectra shown in Fig. 3, the normalized intensities of the peaks associated with the chlorophenyl negative ions, $C_6H_4Cl^-$ ($m/z = 111$), show a clear dependence on the isomeric structure. The intensity ratios of this peak of 1.0:2.5:16.9 for Cs targets and 1.0:1.9:11.4 for K targets of *o*-, *m*-, and *p*-isomers are assumed to reflect the ratios of the relative cross-sections for negative ion formation from the corresponding isomeric chlorophenyl radicals, σ_{nega}.

The order of the peak intensities associated with the isomeric $C_6H_4Cl^-$ ions in the charge inversion spectra of *o*-, *m*-, and *p*-isomers has an inverse relation to that of the electron affinities. Therefore, the apparent dependence of the cross-section σ_{nega} on isomeric structure cannot be explained solely on the basis of the respective vertical electron affinities calculated in the present work. The cross-sections of the negative ion formation are expected to be influenced by many factors other than electron affinity. For example, although the electron affinity of the chlorine atom of 3.617 eV [60] is much larger than those of the chlorophenyl radicals, the peak intensity of the Cl^- ions is much weaker than that of the $C_6H_4Cl^-$ ions in the charge inversion spectra of *p*-dichlorobenze shown in Fig. 2f. The chlorophenyl radical may be vibrationally and rotationally excited because, as seen in Fig. 5, the near-resonant energy levels of the excited dichlorobenzenes are higher than the respective energy levels of the fragments ($C_6H_4Cl^\bullet + Cl^\bullet$). The large structural difference between the radical and anion may also influence the cross-section for negative ion formation for the *o*-isomer.

4. Conclusions

In the charge inversion spectra of $C_6H_4Cl_2^+$ ions produced from *o*-, *m*-, and *p*-dichlorobenzenes, the dominant peaks are those at $m/z = 35$ associated with Cl^- ions, and at $m/z = 111$ associated with $C_6H_4Cl^-$ ions, and the isomeric dependence of the relative intensities of the peaks at $m/z = 35$ and 111 provides a means of clearly discriminating among the *ortho*-, *meta*-, and *para*-isomers of dichlorobenzene ($C_6H_4Cl_2$). The chlorine radical (Cl) and chlorophenyl radical (C_6H_4Cl) are complementary fragments from the dissociation of the excited $C_6H_4Cl_2$ molecules, so the abundance of these fragments is independent of the isomeric form of the precursor. Therefore, in order to compare the normalized intensities of negative ions from positive ions in the charge inversion processes, the intensity of the charge inversion spectra were normalized to the intensity of the peak associated with the relevant precursor $C_6H_4Cl_2^+$ ion. In the normalized spectra, the intensities of the peaks associated with Cl^- ions are almost same for each of the isomers, whereas the intensities of the peaks associated with the $C_6H_4Cl^-$ ions display a clear dependence on the isomeric structure of the precursor. This experimental result can only be explained on the basis that the C_6H_4Cl radicals formed from $C_6H_4Cl_2$ through loss of a Cl atom cannot isomerize, and that the electron transfer cross-sections to form the corresponding negative ions depend on the isomer. The dissociation energies of the C–Cl bond in $C_6H_4Cl_2$, the activation barriers to chlorophenyl radical isomerization, and the electron affinities of the chlorophenyl radicals were calculated by *ab initio* and DFT methods. The large values calculated for the energy barriers for the forward pathways of the isomerization from *o*- to *m*-chlorophenyl radical and from *m*- to *p*-chlorophenyl radical are rationalized by the results of theoretical calculations which indicate that deformation of a bridging hydrogen atom out of plane of the benzene ring is required for isomerization to occur.

Isomeric dependence of the calculated vertical electron affinities was unable to explain satisfactorily the dependence of the peak intensity of the $C_6H_4Cl^-$ ions on the structural isomers in the charge inversion spectra of $C_6H_4Cl_2^+$ ions. The reason for this might be that the cross-sections for negative ion formation from isomeric chlorophenyl ($C_6H_4Cl^\bullet$) radicals in the charge inversion spectrometer are likely to be influenced by the geometrical distortions predicted to occur in this process, as well as possible vibrational and rotational excitation of the chlorophenyl radicals. Nevertheless, the good agreement between the experimental data and the theoretical calculations obtained in this work provides compelling evidence for the existence of isomeric chlorophenyl ($C_6H_4Cl^\bullet$) radicals.

Acknowledgement

We gratefully acknowledge the support of Library & Science Information Center, Osaka Prefecture University for the computational study.

References

[1] M.P. Esposito, H.M. Drake, J.A. Smith, T.W. Owens, United States Environmental Protection Agency Research Reporting Series, (EPA-600/2-80-156) Dioxins, vol. I. Source, Exposure, Transport, and Control, National Technical Information Service, Springfield, 1980.
[2] A. Poland, E. Glover, A.S. Kende, J. Biol. Chem. 251 (1976) 4936.
[3] E.E. McConnell, J.A. Moore, Toxicol. Appl. Pharmacol. 37 (1976) 146.
[4] G. Choudhary, L.H. Keith, C. Rappe (Eds.), Chlorinated Dioxins and Dibenzofurans in the Total Environment, Butterworth, Boston, 1983.
[5] S. Safe, O. Hutzonger, T.A. Hill (Eds.), Polychlorinated Dibenzo-*p*-dioxins and -furans (PCDDs/PCDFs): Sources and Environmental Impact, Epidemiology, Mechanisms of Action, Health Risks, Springer-Verlag, Berlin, 1990.
[6] A. Schecter (Ed.), Dioxins and Health, Plenum, New York, 1994.

[7] J.P. Crine (Ed.), Hazards, Decontamination, and Replacement of PCB: A Comprehensive Guide, Plenum, New York, 1988.
[8] J. Mes, Bull. Environ. Contam. Toxicol. 48 (1992) 815.
[9] R.H. Hill Jr., D.L. Ashley, S.L. Head, L.L. Needham, J.L. Pirkle, Arch. Envioron. Health 50 (1995) 277.
[10] C.J.H. Miermans, L.E. van der Velde, P.C.M. Frintrop, Chemospere 40 (2000) 39.
[11] United States Environmental Protection Agency (EPA 821-B-94-005) Method 1613 Revision B: Tetra- through Octa-chlorinated Dioxines and Furans by Isotope Dilution HRGC/HRMS, EPA, Washington, 1994.
[12] K.L. Busch, G.L. Glish, S.A. McLuckey, Mass Spectrometry/Mass Spectrometry: Technique and Application of Tandem Mass Spectrometry, VCH, New York, 1988 (Chapter 6.1).
[13] D.J. Harvan, J.R. Hass, J.L. Schroeder, B.J. Corbett, Anal. Chem. 53 (1981) 1755.
[14] R.D. Voyksner, J.R. Hass, G.W. Sovocool, M.M. Bursey, Anal. Chem. 55 (1983) 744.
[15] B. Shushan, J.E. Fulford, B.A. Thomson, W.R. Davidson, L.M. Danylewych, A. Ngo, S. Nacson, S.D. Tanner, Int. J. Mass Spectrom. Ion Phys. 46 (1983) 225.
[16] J.B. Plomley, R.E. March, R.S. Mercer, Anal. Chem. 68 (1996) 2345.
[17] R.E. March, M. Splendore, E.J. Reiner, R.S. Mercer, J.B. Plomely, D.S. Waddell, K.A. MacPherson, Int. J. Mass Spectrom. 197 (2000) 283.
[18] S. Hayakawa, K. Taguchi, R. Kotani, K. Arakawa, N. Morishita, J. Mass Spectrom. Soc. Jpn. 49 (2001) 219.
[19] S. Hayakawa, J. Mass Spectrom. 39 (2001) 111.
[20] S. Hayakawa, Y. Kawamura, Y. Takahashi, Int. J. Mass Spectrom. 246 (2005) 56.
[21] S. Hayakawa, K. Harada, K. Arakawa, N. Morishita, J. Chem. Phys. 112 (2000) 8432.
[22] S. Hayakawa, K. Harada, N. Watanabe, K. Arakawa, N. Morishita, Int. J. Mass Spectrom. 202 (2000) A1.
[23] S. Hayakawa, Int. J. Mass Spectrom. 212 (2001) 229.
[24] T. Ichimura, Y. Mori, H. Shinohara, N. Nishi, J. Chem. Phys. 107 (1997) 835.
[25] R.S. Zhu, H. Zhang, G.J. Wang, X.B. Gu, K.L. Han, G.Z. He, N.Q. Lou, Chem. Phys. 248 (1999) 285.
[26] B. Ruscic, L. Klasinc, A. Wolf, J.V. Knop, J. Phys. Chem. 85 (1981) 1486.
[27] S. Fujisawa, I. Oonishi, S. Masuda, K. Ohno, Y. Harada, J. Phys. Chem. 95 (1991) 4250.
[28] F. Muntean, L. Heumann, P.B. Armentrout, J. Chem. Phys. 116 (2002) 5593.
[29] V.G. Zakrzewski, J.V. Ortiz, J. Phys. Chem. 100 (1996) 13979.
[30] J. Cioslowski, G. Liu, D. Moncrieff, J. Phys. Chem. A 101 (1997) 957.
[31] J.K. Terlouw, H. Schwarz, Angew. Chem. Int. Ed. Engl. 26 (1987) 805.
[32] C. Wesdemiotis, F.W. McLafferty, Chem. Rev. 87 (1987) 485.
[33] J.L. Holmes, Mass Specrtom. Rev. 8 (1989) 513.
[34] F.W. McLafferty, Science 247 (1990) 925.
[35] (a) F. Tureček, Org. Mass Spectrom. 27 (1992) 1087;
(b) F. Tureček, J. Mass Spectrom. 33 (1998) 779.
[36] F.W. McLafferty, Int. J. Mass Spectrom. Ion Process. (118/119) (1992) 221.
[37] N. Goldberg, H. Schwarz, Acc. Chem. Res. 27 (1994) 347.
[38] (a) D.V. Zagorevskii, J.L. Holmes, Mass Spectrom. Rev. 13 (1994) 133;
(b) D.V. Zagorevskii, J.L. Holmes, Mass Spectrom. Rev. 18 (1999) 87.
[39] M.J. Polce, S. Beranova, M.J. Nold, C. Wesdemiotis, J. Mass Spectrom. 37 (1996) 1073.
[40] C.A. Schalley, G. Hornung, D. Schröder, H. Schwarz, Chem. Soc. Rev. 27 (1998) 91.
[41] P. Gerbaux, C. Wentrup, R. Flamang, Mass Spectrom. Rev. 19 (2000) 367.
[42] F. Tureček, Top. Curr. Chem. 225 (2003) 77.
[43] G. Hornung, C.A. Schalley, M. Dieterle, D. Schröder, H. Schwarz, Chem. Eur. J. 3 (1997) 1866.
[44] C.A. Schalley, G. Hornung, D. Schröder, H. Schwarz, Int. J. Mass Spectrom. Ion Process. 172 (1998) 181.
[45] D. Schröder, H. Schwarz, S. Dua, S.J. Blanksby, J.H. Bowie, Int. J. Mass Spectrom. 188 (1999) 17.
[46] S. Hayakawa, M. Takahashi, K. Arakawa, N. Morishita, J. Chem. Phys. 110 (1999) 2745.
[47] S. Hayakawa, K. Tomozawa, T. Takeuchi, K. Arakawa, N. Morishita, Chem. Phys. Phys. Chem. 5 (2003) 2386.
[48] S. Hayakawa, N. Kabuki, Eur. Phys. J. D 38 (2006) 163.
[49] S. Hayakawa, H. Endoh, K. Arakawa, N. Morishita, T. Sugiura, Int. J. Mass Spectrom. Ion Process. 151 (1995) 89.
[50] (a) M.J. Frisch, G.W. Trucks, H.B. Schlegel, G.E. Scuseria, M.A. Robb, J.R. Cheeseman, V.G. Zakrzewski, J.A. Montgomery Jr., R.E. Stratmann, J.C. Burant, S. Dapprich, J.M. Millam, A.D. Daniels, K.N. Kudin, M.C. Strain, O. Farkas, J. Tomasi, V. Barone, M. Cossi, R. Cammi, B. Mennucci, C. Pomelli, C. Adamo, S. Clifford, J. Ochterski, G.A. Petersson, P.Y. Ayala, Q. Cui, K. Morokuma, D.K. Malick, A.D. Rabuck, K. Raghavachari, J.B. Foresman, J. Cioslowski, J.V. Ortiz, B.B. Stefanov, G. Liu, A. Liashenko, P. Piskorz, I. Komaromi, R. Gomperts, R.L. Martin, D.J. Fox, T. Keith, M.A. Al-Laham, C.Y. Peng, A. Nanayakkara, C. Gonzalez, M. Challacombe, P.M.W. Gill, B.G. Johnson, W. Chen, M.W. Wong, J.L. Andres, M. Head-Gordon, E.S. Replogle, J.A. Pople, Gaussian 98, Revision A.7, Gaussian Inc., Pittsburgh, PA, 1998;
(b) M.J. Frisch, G.W. Trucks, H.B. Schlegel, G.E. Scuseria, M.A. Robb, J.R. Cheeseman, J.A. Montgomery Jr., T. Vreven, K.N. Kudin, J.C. Burant, J.M. Millam, S.S. Iyengar, J. Tomasi, V. Barone, B. Mennucci, M. Cossi, G. Scalmani, N. Rega, G.A. Petersson, H. Nakatsuji, M. Hada, M. Ehara, K. Toyota, R. Fukuda, J. Hasegawa, M. Ishida, T. Nakajima, Y. Honda, O. Kitao, H. Nakai, M. Klene, X. Li, J.E. Knox, H.P. Hratchian, J.B. Cross, C. Adamo, J. Jaramillo, R. Gomperts, R.E. Stratmann, O. Yazyev, A.J. Austin, R. Cammi, C. Pomelli, J.W. Ochterski, P.Y. Ayala, K. Morokuma, G.A. Voth, P. Salvador, J.J. Dannenberg, V.G. Zakrzewski, S. Dapprich, A.D. Daniels, M.C. Strain, O. Farkas, D.K. Malick, A.D. Rabuck, K. Raghavachari, J.B. Foresman, J.V. Ortiz, Q. Cui, A.G. Baboul, S. Clifford, J. Cioslowski, B.B. Stefanov, G. Liu, A. Liashenko, P. Piskorz, I. Komaromi, R.L. Martin, D.J. Fox, T. Keith, M.A. Al-Laham, C.Y. Peng, A. Nanayakkara, M. Challacombe, P.M.W. Gill, B. Johnson, W. Chen, M.W. Wong, C. Gonzalez, J.A. Pople, Gaussian 03, Revision B.05, Gaussian Inc., Pittsburgh, PA, 2003.
[51] W.J. Hehre, L. Radom, P.v.R. Schleyer, P.A. Pople, Ab Initio Molecular Orbital Theory, Wiley, New York, 1986.
[52] S. Hayakawa, Int. J. Mass Spectrom. Ion Process. 90 (1989) 251.
[53] S. Hayakawa, N. Terazawa, T. Sugiura, J. Phys. B 23 (1990) 4539.
[54] S. Hayakawa, A. Matsumoto, M. Yoshioka, T. Sugiura, Rev. Sci. Instrum. 63 (1992) 1958.
[55] S. Hayakawa, Int. J. Mass Spectrom. Ion Process. 116 (1992) 167.
[56] S. Hayakawa, N. Terazawa, T. Sugiura, J. Mass Spectrom. Soc. Jpn. 41 (1993) 225.
[57] S. Hayakawa, K. Kadomura, K. Fujii, J. Mass Spectrom. Soc. Jpn. 43 (1995) 239.
[58] V.H. Wysocki, H.I. Kenttämaa, R.G. Cooks, Int. J. Mass Spectrom. Ion Process. 75 (1987) 181.
[59] P.G. Wenthold, R.R. Squires, W.C. Lineberger, J. Am. Chem. Soc. 120 (1998) 5279.
[60] S.G. Lias, J.E. Bartmess, J.F. Liebman, J.L. Holmes, R.D. Levin, W.G. Mallard, J. Phys. Chem. Ref. Data 17 (Suppl. 1) (1988).
[61] CASSCF(6.6)/6-31 + G(d,p) calculation also carried out and provided the lowest vertical excitation energy of 4.910 eV for singlet state of *o*-dichlorobenzene, which is good agreement with the TD-B3LYP calculation.
[62] S.W. Benson, F.R. Cruickshank, D.M. Golden, G.R. Haugen, H.E. O'Neal, A.S. Rodgens, R. Shaw, R. Walsh, Chem. Rev. 69 (1969) 279.
[63] S. Hayakawa, K. Kadomura, M. Kimura, C.M. Dutta, Phys. Rev. A 70 (2004) 022708.